# Novel Optical Material: Polyarylates with Heterocyclic Side Chain Groups

I. ZADROŻNA,[1] P. PARZUCHOWSKI,[1] Z. K. BRZOZOWSKI,[1] G. H. W. MILBURN[2]

[1] Warsaw University of Technology, Department of Speciality Polymers, Koszykowa 75, 00-662 Warsaw, Poland

[2] Napier University, Edinburgh, United Kingdom

*Received 12 June 1997; accepted 11 April 1998*

**ABSTRACT:** Several nonlinear optical polymers containing azometine side-chain groups have been obtained by interfacial polycondensation. The structures of obtained monomers and polymers were confirmed by infrared, $^1$H-NMR, and ultraviolet spectroscopies. Mechanical, thermal, and optical properties of the obtained polymers were evaluated. The investigations show that some of the new polymers obtained in this study may find use in optical applications. © 1999 John Wiley & Sons, Inc. J Appl Polym Sci 71: 1017–1028, 1999

**Key words:** polyarylates; NLO materials; Schiff bases; heterocyclic systems

## INTRODUCTION

It has been several years since the first electric field poled second-order nonlinear polymers have been reported.[1] During this period a wide variety of polymeric systems have been formulated and investigated. Several reviews have concentrated on a variety of polymer systems including guest-host systems, side-chain polymers, main-chain polymers and cross-linked systems produced by thermal and photochemical methods with different chromophores.[2,3] Allen and co-workers carried out the synthesis of amorphous polymers with a variety of side groups, substituting typical electronaccepting groups (like nitro groups) with stronger electronaccepting groups such as benzothiazoles, benzimidazoles and benzoxazoles.[4]

For several years our group has conducted photopolymer research.[5–9] Several polyarylates based on bisbenzylidenoketones were investigated as potential second-order nonlinear polymers.[10–13]

The subject of this article is the synthesis of polyarylates based on special monomer Schiff's bases obtained from the condensation reaction between 2,4-dihydroxy benzaldehyde and formylbisphenol and 4 or 5 substituted 2-aminothiazoles and having potential second-order nonlinear properties. The structures of the monomers obtained and the polyarylates were investigated by infrared (IR), $^1$H-NMR, and ultraviolet (UV) spectroscopy. Some mechanical and optical properties of the polyarylates were also investigated. Our materials were designed to be potential second-order nonlinear polymers and materials for use in practical systems as frequency doublers and in electrooptic devices.

## EXPERIMENTAL

IR spectra were recorded from 4000 to 700 cm$^{-1}$ on a Specord M-80 Carl-Zeiss with KBr pellets. NMR spectra were recorded on a Gemini 200 spectrometer in $d_6$-DMSO. UV-vis spectra were recorded with a Perkin–Elmer Lambda 2 spectrophotometer from 190 to 800 nm in dichloromethane. The polymer tensile strength was measured

---

*Correspondence to:* I. Zadrożna.

Journal of Applied Polymer Science, Vol. 71, 1017–1028 (1999)
CCC 0021-8995/99/061017-12

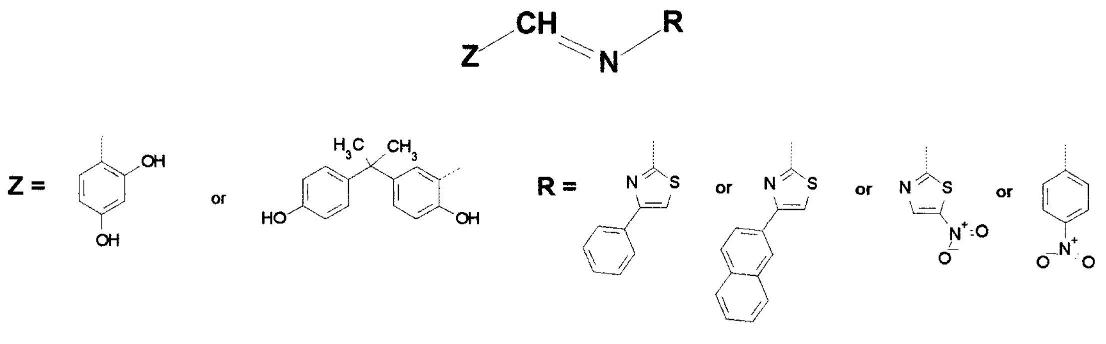

1 2 a b c d

**Figure 1** Formula scheme of synthesized monomers.

according to the Polish Standard PN-81 C-89034. We used ten 1-cm polymer film strips. Tensile strength is given by

$$\sigma = \frac{F_{\max}}{A_0}, \tag{1}$$

where $F_{\max}$ is the maximum tensile force, $N$, and $A_0$ is the cross-sectional area ($m^2$). The intrinsic viscosity was determined by an Ostwald viscosimeter.[14]

### Monomer Synthesis

For interfacial polycondensation reactions we used several special imine monomers, derivatives of substituted amino thiazoles of the general formula presented in Figure 1. Synthesis of the monomers was carried out using the condensation reaction between the carbonyl compound (2,4-dihydroxybenzaldehyde or formylbisphenol A) and the amine in a refluxing solvent (ethanol or xylene).

The formyl derivative of bisphenol A was synthesized using the Reimer–Tiemann procedure for phenol formylation.[15] In the Reimer–Tiemann reaction chloroform and hydroxide ions are used to formylate aromatic rings. The attacking entity in this reaction is dichlorocarbene $:CCl_2$. This is known to be produced by the treatment of chloroform with bases.

Dichlorocarbene effects electrophilic substitution in the reactive phenolate ions, giving the benzylidene dichloride hydrolized by the alkaline medium to the corresponding hydroxyaldehyde. The phenolic aldehyde is isolated from the reaction mixture after acidification.

After 28 g (0.7 mol) NaOH is dissolved in 60 mL of water, 19.8 g (0.087 mol) of bisphenol A is added. The reaction mixture is heated to 70°C, at which point all of the bisphenol is dissolved. The reaction is carried out in an atmosphere of argon. Chloroform 26.5 mL (39.12 g, 0.34 mol) is added dropwise with vigorous stirring for 3 h. The temperature is kept at 60–70°C. The color of the mixture changes from light yellow to dark red. After the entire amount of chloroform is added, the reaction is slowly cooled to room temperature and the product precipitated with dilute sulphuric acid. The crude product is purified by column

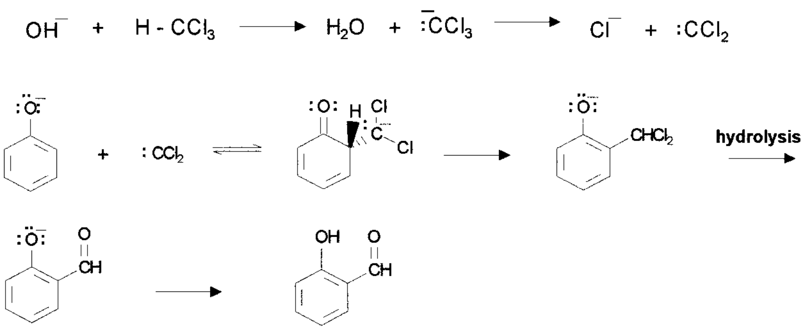

**Scheme 1** Reimer–Tiemann reaction mechanism.

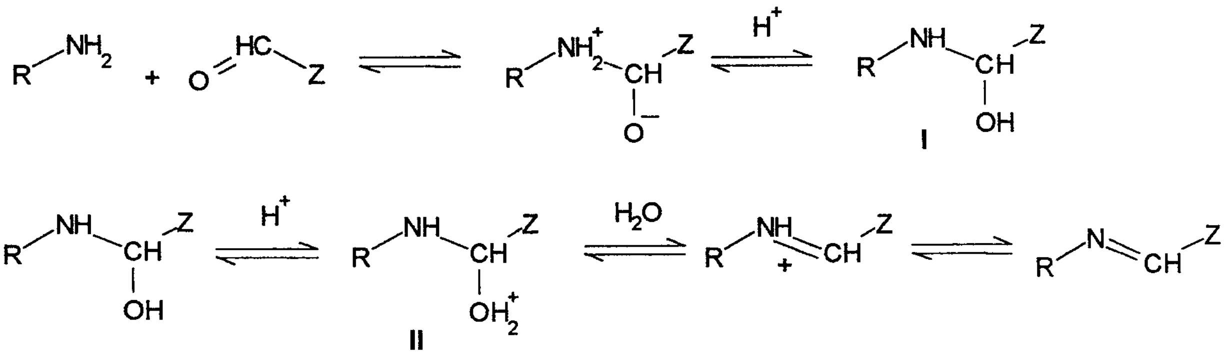

**Scheme 2** Schiff bases formation mechanism for primary amine and an aldehyde.

chromatography. In addition to the main product, monoformyl bisphenol A, the crude product also contains unreacted bisphenol A and diformyl bisphenol A.

Aldehydes react readily with both alkylamines and arylamines to give compounds known as imines or Shiff bases. Usually, heating the aldehyde and the amine together while distilling off the water that forms leads to the product. The reaction is reversible; imines can be converted back into aldehydes and amines by reaction with water. Imines are stable enough for isolation. However, they can decompose or polymerize (especially when substituted with simple R groups) unless there is at least one aryl group on the nitrogen or the carbon.

Slow reactions can be catalyzed by acids, usually *p*-toluenesulphonic acid. The mechanism of the reaction is generally expressed as shown in Scheme 2.

In the acid-catalyzed reaction, presumably the *N*-hemiacetal (**I**) is protonated to (**II**). The actual rate of enamine formation depends in a complex way on several factors:

- the basicity of the amine
- the degree of steric hindrance in either the amine or the aldehyde, which affects the rate of formation of **I**
- the rate of loss of the hydroxyl group from **I**
- the rate of loss of a proton from **II.**

A solution of an amine and 5% molar excess of an appropriate aldehyde in ethanol (1a, 2a; see Fig. 1) or in xylene (1b, 1c, 2b, 2d; Fig. 1) was heated under reflux for 10 h. Reactions carried out in xylene needed catalytic amounts of *p*-toluenesulphonic acid. Products 1a and 2a were purified by recrystallization. Other products were purified by column chromatography. The reaction was reversible, and the crude product contained unreacted starting compounds that were difficult to remove by recrystallization.

### Polymer Synthesis

Copolyarylates can be obtained via interfacial polycondensation[16,17] from the special monomers and bisphenol A. The reaction conditions used were as follows. The water phase contained bisphenols in alkali solution and catalyst. As a catalyst, we used TEBA$^+$Cl$^-$ chloride (triethylbenzylammonium chloride) 5 mol % relative to the bisphenol concentration. The reaction was carried out at room temperature. The time of addition of acid chloride mixtures in methylene chloride (organic phase) was 5 min. The mixture of terephthalic and isophthalic acid chlorides was used in an optimal ratio of 2 : 1.

After 2 h of stirring at a rate of about 1500 rpm, additional methylene chloride was added to dilute the reaction mixture. After another 1 h of stirring, the whole system was acidified. The organic phase was separated, washed with distilled water, and dropped into vigorously stirred acetone. The polymer that precipitated in acetone was filtered, washed with acetone, and dried. General schematic formulas for polyarylates are given in Figure 3.

Monomer 1a was used in 1, 2, 4, 6, and 10 mol % concentrations in reactions with bisphenol A. Monomers 1b, 2a, and 2b were used at 1 and 2 mol %, and monomers 1c and 2d were used at 1 mol % with bisphenol A. To compare the results, synthesis of polyarylate without special monomers was performed.

In cases where monomers 1a, 1b, 2a, and 2b were used, light yellow polymers were obtained.

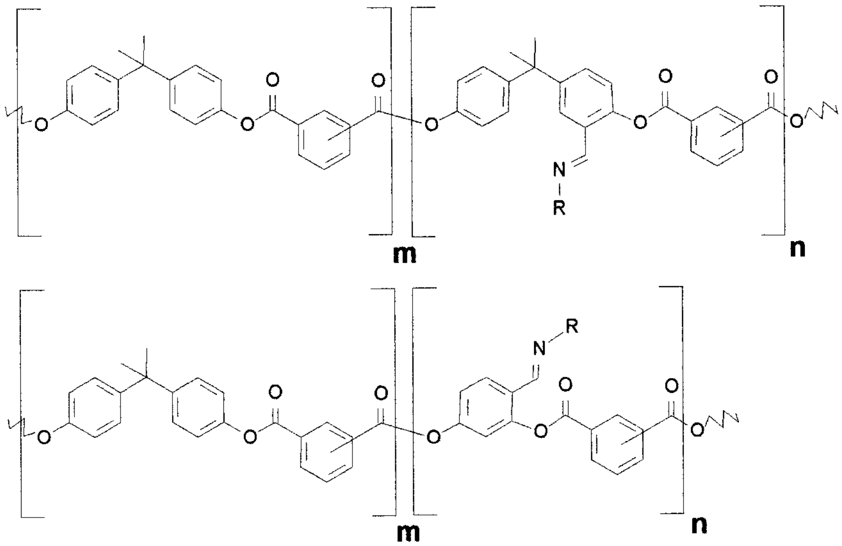

**Figure 2** General formulas for polyarylates. $R$ as defined in Figure 1; **m, n** = 1, 2, 3 . . .

Polycondensation using monomers 1c and 2d and without special monomers yielded white polymers. This shows that hydrolysis of 1c and 2d occurred during polycondensation reactions.

### Polymer Investigation Methods

Polyarylate films were obtained by pouring a polymer solution in dichloromethane onto a levelled glass plate placed in glass chamber. The concentration of the solution was 8 g polymer/100 $cm^3$ solvent. Films were obtained by slow evaporation of the solvent. Thin films for optical measurements were obtained in a similar way. To avoid thickness differences of the polymer film, a glass plate was placed in a levelled vessel containing polymer solution, below the solution surface. The concentration of a polymer in dichloromethane was fixed empirically and depended on the glass plate's height and the vessel's surface. The vessel was placed in a glass chamber to avoid dust, and the solvent was allowed to evaporate very slowly.

## RESULTS AND DISCUSSION

### Formyl Bisphenol Structures

### $^1$H-NMR Spectra

2-(4-hydroxyphenyl)-2′-(3-formyl-4-hydroxyphenyl)-propane; yield 50%.

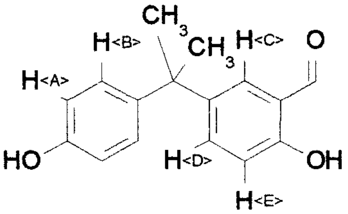

$\delta$ = 1.66 (s, 6H, $CH_3$); 4.50 (bs, 1H, OH); 6.73–6.78 (m, $2H_A$, Ar); 6.89 (d, $1H_E$, $J$ = 8.66 Hz); 7.06–7.11 (m, $2H_B$, Ar); 7.37 (dd, $1H_D$, $J$ = 2.47 Hz, $J$ = 8.66 Hz); 7.43 (d, $1H_C$, $J$ = 8.66 Hz); 9.84 (s, 1H, CH═O); 10.93 (s, 1H, $OH_{asoc.}$).

2,2′-di(3-formyl-4-hydroxyphenyl)propane; yield 5%.

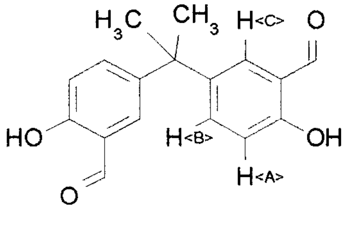

$\delta$ (ppm) = 1.70 (s, 6H, $CH_3$); 6.91 (d, $2H_A$, $J$ = 8.75 Hz); 7.34 (dd, $2H_B$, $J$ = 2.49 Hz, $J$ = 8.75 Hz); 7.44 (d, $2H_C$, $J$ = 2.49 Hz); 9.85 (s, 2H, CH═O); 10.94 (s, 2H, $OH_{asoc.}$).

The IR spectra of formyl derivatives of bisphenol A shows the characteristic OH band (at 3400 $cm^{-1}$) and valence vibratons characteristic of a C═O band (at 1650 $cm^{-1}$).

MS: 256, 241, 213, 197, 181, 165, 147, 119, 107, 91, 65, 51, 39 m/z.

## Monomer Structures

2-(2,4-dihydroxybenzylidenoamino)-4-phenylothiazole (**1a;** see Fig. 1); yield 58%.

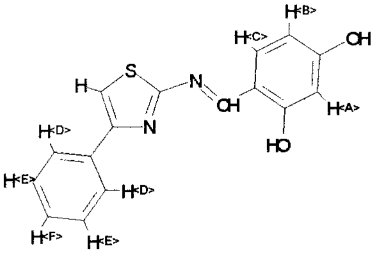

$^1$H-NMR: $\delta = 6.43$ (d, $1H_A$, $J = 2.29$ Hz); 6.53 (dd, $1H_B$, $J = 2.29$ Hz, $J = 8.58$ Hz); 7.30–7.49 (m, $3H_{E,F}$, Ar); 7.60 (d, $1H_C$, $J = 8.58$ Hz); 7.80 (s, 1H, $=C\underline{H}-S$); 7.99–8.04 (m, $2H_D$, Ar); 9.28 (s, 1H, $C\underline{H}=N$); 9.51 (bs, 1H, $O\underline{H}$); 12.62 (bs, 1H, $O\underline{H}_{asoc.}$). IR: (KBr) = 3460 ($\nu$OH) cm$^{-1}$; 1632 ($\nu$C=N) cm$^{-1}$. UV: ($CH_2Cl_2$) $\lambda_{max}$ = 230, 290, 390 nm.

2-(2,4-dihydroxybenzylidenoamino)-4-(2-naphthylo)thiazole (**1b;** see Fig. 1); yield 56%.

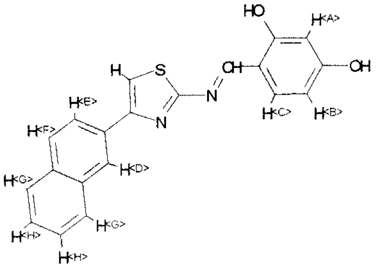

$^1$H-NMR: $\delta = 6.38$ (d, $1H_A$, $J = 2.02$ Hz); 6.47 (dd, $1H_B$, $J = 2.02$ Hz, $J = 8.39$ Hz); 7.51–7.55 (m, $2H_{E,F}$, Ar); 7.71 (d, $1H_C$, $J = 8.39$ Hz); 7.90–8.13 (m, $4H_{G,H}$, Ar); 8.10 (s, 1H, $=C\underline{H}-S$); 8.53 (s, $1H_D$, Ar); 9.24 (s, 1H, $C\underline{H}=N$); 10.60 (bs, 1H, $O\underline{H}$); 12.01 (bs, 1H, $O\underline{H}_{asoc.}$). IR: (KBr) = 3440 ($\nu$OH) cm$^{-1}$; 1634 ($\nu$C=N) cm$^{-1}$.

2-(2,4-dihydroxybenzylidenoamino)-5-nitrothiazole (**1c;** see Fig. 1); yield 59%.

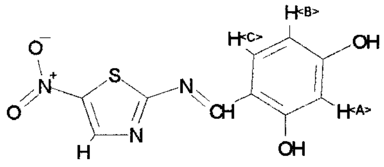

$^1$H-NMR: $\delta = 6.37$ (d, $1H_A$, $J = 1.81$ Hz); 6.45 (dd, $1H_B$, $J = 1.81$ Hz, $J = 8.72$ Hz); 7.76 (d, $1H_C$, $J = 8.72$ Hz); 8.68 (s, 1H, $N-C\underline{H}=$); 9.24 (s, 1H, $C\underline{H}=N$); 10.88 (bs, 1H, $O\underline{H}$); 11.50 (bs, 1H, $O\underline{H}$). IR: (KBr) = 3440 ($\nu$OH) cm$^{-1}$; 1634 ($\nu$C≡N) cm$^{-1}$; 1522, 1336 ($\nu NO_2$) cm$^{-1}$.

2-{3-[(4-phenyl-2-thiazolil)iminomethyl]-4-hydroxyphenyl}-2-(4-hydroxyphenyl)propane (**2a;** see Fig. 1); Yield 60%.

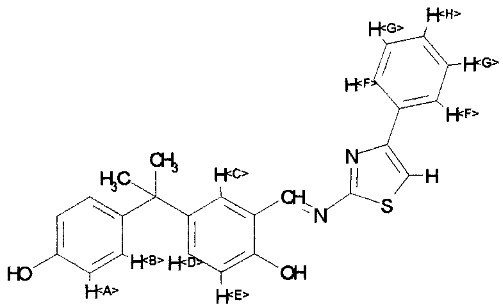

$^1$H-NMR: $\delta = 1.60$ (bs, 6H, $C\underline{H}_3$); 6.62–6.68 (m, $2H_A$, Ar); 6.90 (d, $1H_E$, $J = 8.87$ Hz); 7.00–7.04 (m, $2H_B$, Ar); 7.24 (dd, $1H_D$, $J = 2.38$ Hz, $J = 8.87$ Hz); 7.31–7.49 (m, $3H_{G,H}$, Ar); 7.83 (d, $1H_C$, $J = 2.38$ Hz); 7.96–7.99 (m, $2H_F$, Ar); 8.03 (s, 1H, $=C\underline{H}-S$); 9.18 (bs, 1H, $O\underline{H}$); 9.36 (s, 1H, $C\underline{H}=N$); 11.41 (bs, 1H, $O\underline{H}_{asoc.}$). IR: (KBr) = 3315 ($\nu$OH) cm$^{-1}$; 1616 ($\nu$C=N) cm$^{-1}$. IR: ($CHCl_3$) = 3600 ($\nu$OH) cm$^{-1}$; 3320 ($\nu OH_{asoc.}$) cm$^{-1}$; 1616 ($\nu$C=N) cm$^{-1}$.

2-(3-{[4-(2-naphthyl)-2-thiazolil]iminomethyl}-4-hydroxyphenyl)-2-(4-hydroxyphenyl)propane (**2b;** see Fig. 1); Yield 46%.

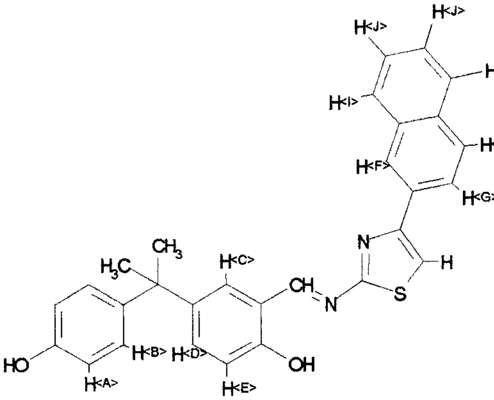

$^1$H-NMR: $\delta = 1.60$ (bs, 6H, $C\underline{H}_3$); 6.64–6.68 (m, $2H_A$, Ar); 6.66 (d, $1H_E$, $J = 8.66$ Hz); 6.99–7.05 (m, $2H_B$, Ar); 7.26 (dd, $1H_D$, $J = 2.24$ Hz, $J = 8.66$ Hz); 7.50–7.55 (m, $2H_{G,H}$, Ar); 7.84 (d, $1H_C$, $J = 2.24$ Hz); 7.90–8.13 (m, $4H_{I,J}$, Ar); 8.17 (s, 1H, $=C\underline{H}-S$); 8.53 (bs, $1H_F$, Ar); 9.38 (s, 1H, $C\underline{H}=N$); 10.21 (bs, 1H, $O\underline{H}$); 11.20 (bs, 1H, $O\underline{H}$). IR: (KBr) = 3316 ($\nu$OH) cm$^{-1}$; 1615 ($\nu$C=N) cm$^{-1}$. IR: ($CHCl_3$) = 3596 ($\nu$OH) cm$^{-1}$; 3316 ($\nu OH_{asoc.}$) cm$^{-1}$; 1616 ($\nu$C=N) cm$^{-1}$.

2-(4-hydroxyphenyl)-2-{4-hydroxy-3-[(4-nitrophenyl)iminomethyl]phenyl}propane (**2d;** see Fig. 1); Yield 62%.

**Table I Mechanical Properties of Polyarylate Layers**

| Film Symbol | Tensile Strength (MPa) |
|---|---|
| PAr **1a** 1% | 28.17 |
| PAr **1a** 2% | 44.75 |
| PAr **1a** 4% | 34.06 |
| PAr **1a** 6% | 40.90 |
| PAr **1a** 10% | 26.55 |
| PAr **1b** 1% | 42.14 |
| PAr **1b** 2% | 24.20 |
| PAr **1c** 1% | 34.74 |
| PAr **2a** 1% | 35.79 |
| PAr **2a** 2% | 37.11 |
| PAr **2b** 1% | 59.07 |
| PAr **2b** 2% | 33.92 |
| PAr **2d** 1% | 33.81 |
| PAr **0** | 42.19 |

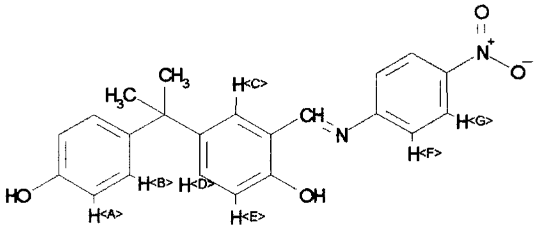

$^1$H-NMR: $\delta$ = 1.57 (bs, 6H, C$\underline{H}_3$); 6.60–6.66 (m, 2H$_A$, Ar); 6.87 (d, 1H$_E$, $J$ = 8.8 Hz); 6.95–7.02 (m, 2H$_B$, Ar); 7.28 (dd, 1H$_D$, $J$ = 2.45 Hz, $J$ = 8.8 Hz); 7.50 (d, 1H$_C$, $J$ = 2.45 Hz); 7.54–7.63 (m, 2H$_F$, Ar); 8.25–8.30 (m, 2H$_G$, Ar); 8.94 (s, 1H, C$\underline{H}$=N); 9.28 (bs, 1H, O$\underline{H}$); 10.19 (bs, 1H, O$\underline{H}$). IR: (film) = 3368 ($\nu$OH) cm$^{-1}$; 1614 ($\nu$C=N) cm$^{-1}$; 1516, 1344 ($\nu NO_2$) cm$^{-1}$.

The yields of the polymers ranged from 65 to 75%.

## Mechanical Properties of Polymer Films

The mechanical properties of the polymer films (values of tensile strengths) are given in Table I. Values of mechanical properties given in Table I have comparative value only. As a standard, the PAr 0 film was selected; this was obtained from a polyarylate synthesized with a bisphenol A base.

All measured films showed good tensile strength. Addition of the special monomers did not cause much decrease in the mechanical properties of polymer films.

## UV-Vis Spectra

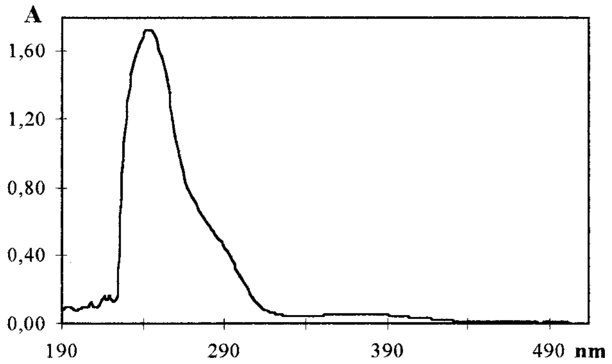

**Figure 3** UV-vis spectrum of the PAr **1a** 10% polymer.

For all polymers, an absorption maximum in the wavelength range of 220–320 nm was observed (Fig. 3). Moreover, it was found that in addition to an increased amount of azometine compound in the mixture, the band intensity at 370 nm is also increased, as shown in Figure 4.

## Determination of Intrinsic Viscosity

Intrinsic viscosity (i.e., limiting viscosity number) was determined by an Ostwald viscosimeter. In each case, obtained values were compared with the intrinsic viscosity of the polymer synthesized on bisphenol A base PAr 0. These results are given in Table II.

## Determination of Thermal Properties of Polymers

Glass temperature ($T_g$) was determined by the differential scanning calorimetry method and was measured for four polymers; results are given in Table III. The polymers show $T_g$ in the range typical for polyarylates. The values of $T_g$ are similar. Changing neither the concentration of the

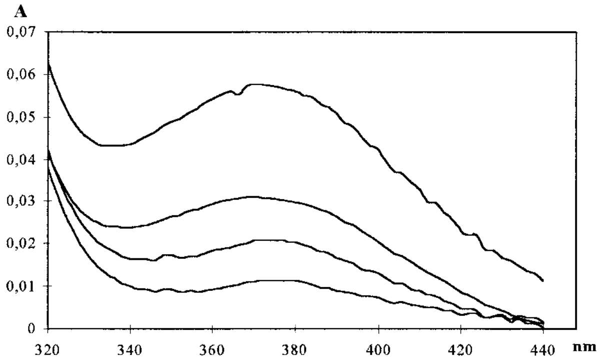

**Figure 4** UV-vis spectra for polymer series PAr1 with varying amounts of the azometine monomer.

**Table II Intrinsic Viscosity of the Polyarylates**

| Polymer | Intrinsic Viscosity ($\eta$) (100 cm$^3$/g) |
|---|---|
| PAr **1a** 1% | 1.65 |
| PAr **1a** 2% | 0.74 |
| PAr **1a** 4% | 1.02 |
| PAr **1a** 6% | 0.74 |
| PAr **1a** 10% | 0.81 |
| PAr **1b** 1% | 0.74 |
| PAr **1b** 2% | 1.14 |
| PAr **1c** 1% | 1.73 |
| PAr **2a** 1% | 1.42 |
| PAr **2a** 2% | 0.77 |
| PAr **2b** 1% | 1.37 |
| PAr **2b** 2% | 1.14 |
| PAr **2d** 1% | 1.98 |
| PAr **0** | 1.11 |

special monomer nor its chemical structure has a remarkable influence on $T_g$. The temperature at the onset of decomposition and the temperature at the fastest decomposition were determined by thermogravimetric analysis.

Thermogravimetric analysis was performed in the presence of air, in the temperature range 25–620°C with a heating rate of 5°C/min. The values of the temperatures at the onset of decomposition and the temperatures at the fastest decompositions are given in Table IV.

All of the polymers showed high thermostability, beginning to decompose only above 310°C. The influence of the amount of special monomer added on thermal stability is seen on the PAr 1a series. Addition of azometine compound 1a caused a decrease in thermic stability from 340°C for PAr **1a** 1% to 310°C for PAr **1a** 10%. Figure 5 shows the beginning of decomposition temperature and the fastest decomposition temperature for all synthesized polymers. Polymers containing formyl bisphenol derivatives (PAr 2a, 2b, and 2d) showed slightly better thermal properties than polymers containing 2,4-dihydroxybenzaldehyde derivatives (PAr 1a, 1b, and 1c).

**Table III Glass Temperatures of Selected Polymers**

| Polymer | Glass Temperature (°C) |
|---|---|
| PAr **1a** 2% | 117.5 |
| PAr **1a** 10% | 123.0 |
| PAr **2a** 2% | 124.5 |
| PAr **2b** 2% | 122.0 |

**Table IV Decomposition Temperatures of the Polymers**

| Polymer | Beginning of Decomposition (°C) | The Fastest Decomposition (°C) |
|---|---|---|
| PAr **1a** 1% | 340 | 520 |
| PAr **1a** 2% | 340 | 460 |
| PAr **1a** 4% | 320 | 460 |
| PAr **1a** 6% | 320 | 450 |
| PAr **1a** 10% | 310 | 440 |
| PAr **1b** 1% | 340 | 460 |
| PAr **1b** 2% | 350 | 480 |
| PAr **1c** 1% | 340 | 500 |
| PAr **2a** 1% | 340 | 460 |
| PAr **2a** 2% | 350 | 470 |
| PAr **2b** 1% | 350 | 460 |
| PAr **2b** 2% | 340 | 480 |
| PAr **2d** 1% | 330 | 480 |
| PAr **0** | 340 | 460 |

## Determination of Thickness and Optical Constants of Polymer Film

The amorphous polymer films that were prepared were designed for use in optical measurements and optical devices. The films had a thickness of ~ 1 $\mu$m, and it is important to know the refractive index $n(\lambda)$ and absorption coefficient $\alpha(\lambda)$ as a function of wavelength to predict their photoelectric behaviour. A procedure has been presented[19] to determine the thickness and optical constants from the interference fringes of the transmission spectrum to an accuracy of better than 1%, provided that the films are of good quality. The theoretical background for all of the calculations has been published before.[19]

Swanepoel presented a very convenient method of determining the thickness and optical constants of amorphous silica film.[19] Here that method was used for calculating thickness and optical constants of thin polyarylate film. The method for preparing polymer films was presented earlier. Transmission spectra were recorded using polymer film on glass substrate. Polymer PAr 1a 2% (see Fig. 1) was used for calculations, but this method can be used for all synthesized polyarylates.

If the thickness $d$ of the film is not uniform or slightly tapered, then all interference effects are

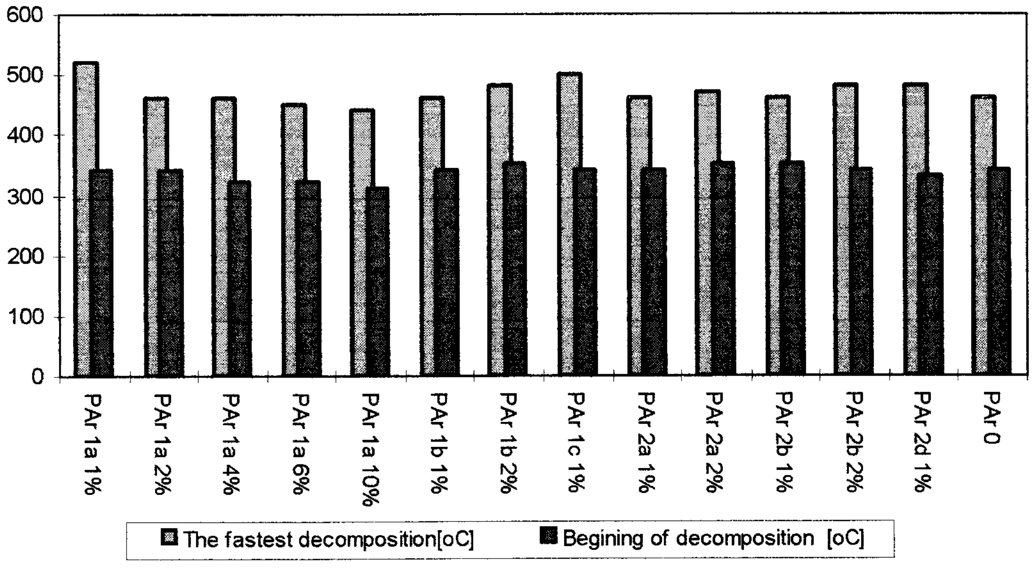

**Figure 5** Thermic resistance of the polymer.

destroyed and the transmission is a smooth curve. If the thickness $d$ is uniform, then interference effects give rise to a spectrum shown by the full curve in Figure 2. Far from being a nuisance, these fringes can be used to calculate the optical constants of the film.

The basic equation for interference fringes is

$$2nd = m\lambda, \tag{2}$$

where $m$ is an integer for maxima and a half-integer for minima. Equation (2) contains information on the product of $n$ and $d$, and there is no way of obtaining information on either $n$ or $d$ separately using this equation only.

The refractive index of the substrate can be determined by measuring the transmission spectrum of the clean substrate alone and using eq. (3) to calculate $s$:

$$s = \frac{1}{T_s} + \left(\frac{1}{T_s^2} - 1\right)^{1/2} \tag{3}$$

In these calculations $s$ is assumed to be constant at a value $s = 1.56$, yielding a transmission of 0.908, as shown by $T_s$ in Figure 7.

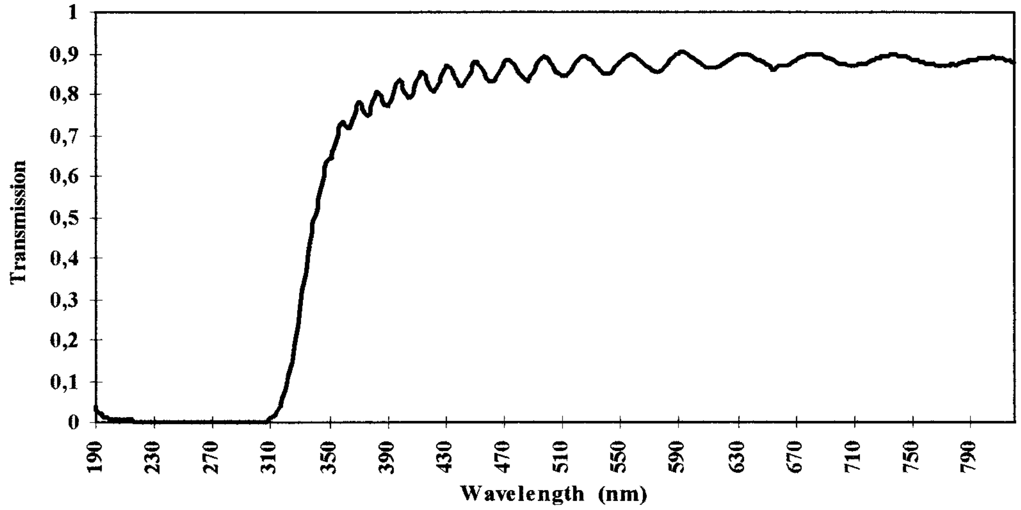

**Figure 6** Transmission spectrum for a PAr **1a** 2% film on a finite glass substrate.

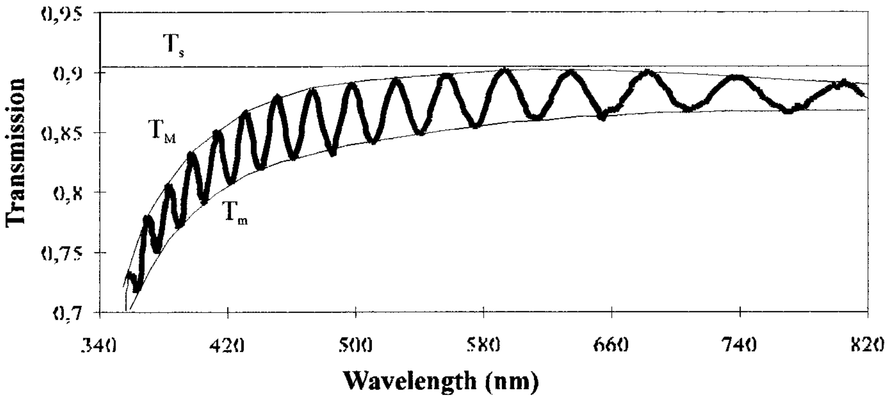

**Figure 7** Interference fringes: $T_s$, $T_M$, and $T_m$ curves.

For calculation of the refractive index $n$, the values of $T_M$ and $T_m$ at different $\lambda$ must be obtained. Table I shows the values at the extremes of the spectrum of $\lambda$, $T_M$, and $T_m$ obtained from Figure 7. The transmission values were read on the curves of $T_M$ and $T_m$ at each wavelength. The intermediate values were calculated by computer, and a linear interpolation was done.

The values of refractive index $n_1$ as calculated from eq. (4) are shown in Table I. The accuracy can be improved after calculating thickness $d$:

$$n = [N + (N^2 - s^2)^{1/2}]^{1/2}, \qquad (4)$$

where

$$N = 2s\frac{T_M - T_m}{T_M T_m} + \frac{s^2 + 1}{2} \qquad (5)$$

The values of $n_1$ in Table I are calculated at the extremes of the spectrum. This value can be calculated at any value of $\lambda$ using the smooth envelopes $T_M$ and $T_m$.

If $n_1$ and $n_2$ are the refractive indexes at two adjacent maxima (or minima) at $\lambda_1$ and $\lambda_2$, then it follows from eq. (1) that the thickness is given by

$$d = \frac{\lambda_1 \lambda_2}{2(\lambda_1 n_2 - \lambda_2 n_1)} \qquad (6)$$

Equation (6) is very sensitive to errors in $n$ and is not very accurate. The values of $d$ calculated from eq. (6) are shown as $d_1$ in Table V. There is some dispersion of the values of $d_1$.

The average value of $d_1$ ignoring the last two values (which were not shown in Table V) is 2572 ± 733 nm. This value of $d_1$ can be now used with $n_1$ to determine the order numbers ($m$) for the

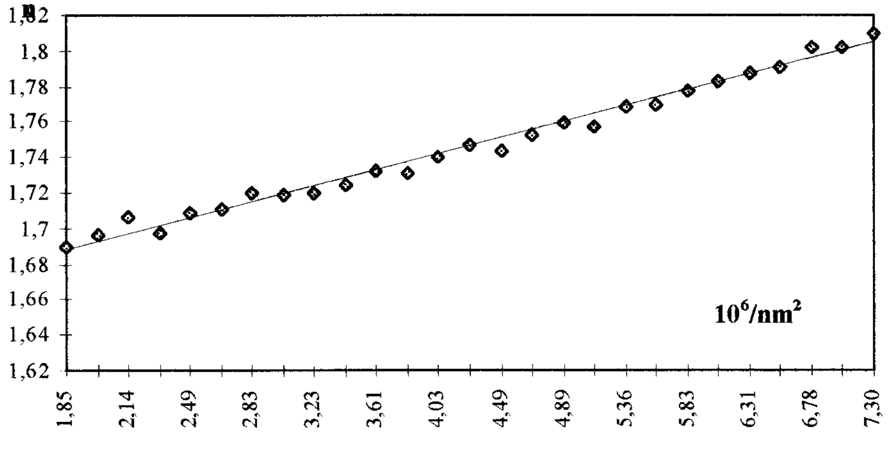

**Figure 8** Plot of $n$ versus $1/\lambda^2$.

**Table V Values of λ, $T_M$, and $T_m$ for the Spectrum of Figure 7; Calculation of $n$ and $d$**

| λ [nm] | $T_M$ | $T_m$ | $n_1$ | $d_1$ | $m$ | $d_2$ | $n_2$ |
|---|---|---|---|---|---|---|---|
| 806 | 0.891 | 0.868 | 1.652 | | 10.5 | 2,561 | 1.690 |
| 774 | 0.893 | 0.868 | 1.660 | | 11 | 2,564 | 1.700 |
| 736 | 0.896 | 0.868 | 1.669 | 2,302 | 11.5 | 2,536 | 1.690 |
| 708 | 0.897 | 0.868 | 1.675 | 2,262 | 12 | 2,536 | 1.696 |
| 684 | 0.899 | 0.864 | 1.695 | 2,371 | 12.5 | 2,522 | 1.707 |
| 654 | 0.899 | 0.860 | 1.709 | 2,020 | 13 | 2,487 | 1.697 |
| 634 | 0.899 | 0.861 | 1.708 | 2,319 | 13.5 | 2,506 | 1.709 |
| 612 | 0.901 | 0.861 | 1.710 | 2,778 | 14 | 2,506 | 1.711 |
| 594 | 0.902 | 0.858 | 1.725 | 2,369 | 14.5 | 2,496 | 1.720 |
| 574 | 0.899 | 0.854 | 1.730 | 2,273 | 15 | 2,489 | 1.719 |
| 556 | 0.897 | 0.852 | 1.731 | 2,397 | 15.5 | 2,489 | 1.721 |
| 540 | 0.895 | 0.849 | 1.733 | 2,544 | 16 | 2,492 | 1.725 |
| 526 | 0.893 | 0.845 | 1.739 | 2,588 | 16.5 | 2,495 | 1.733 |
| 510 | 0.892 | 0.842 | 1.748 | 2,299 | 17 | 2,480 | 1.731 |
| 498 | 0.891 | 0.836 | 1.766 | 2,095 | 17.5 | 2,468 | 1.740 |
| 486 | 0.888 | 0.830 | 1.778 | 2,165 | 18 | 2,460 | 1.747 |
| 472 | 0.885 | 0.829 | 1.771 | 2,410 | 18.5 | 2,465 | 1.743 |
| 462 | 0.881 | 0.829 | 1.762 | 3,210 | 19 | 2,491 | 1.752 |
| 452 | 0.878 | 0.824 | 1.767 | 3,205 | 19.5 | 2,494 | 1.760 |
| 440 | 0.873 | 0.820 | 1.765 | 2,524 | 20 | 2,492 | 1.757 |
| 432 | 0.867 | 0.813 | 1.773 | 2,563 | 20.5 | 2,498 | 1.768 |
| 422 | 0.860 | 0.806 | 1.773 | 2,629 | 21 | 2,498 | 1.769 |
| 414 | 0.852 | 0.799 | 1.774 | 2,767 | 21.5 | 2,509 | 1.777 |
| 406 | 0.842 | 0.793 | 1.768 | 3,293 | 22 | 2,526 | 1.783 |
| 398 | 0.833 | 0.782 | 1.776 | 2,806 | 22.5 | 2,521 | 1.788 |
| 390 | 0.820 | 0.772 | 1.772 | 2,648 | 23 | 2,531 | 1.791 |
| 384 | 0.807 | 0.760 | 1.772 | 3,305 | 23.5 | 2,547 | 1.802 |
| 376 | 0.793 | 0.748 | 1.772 | 2,953 | 24 | 2,546 | 1.802 |
| 370 | 0.780 | 0.733 | 1.786 | 2,360 | 24.5 | 2,538 | 1.810 |
| 364 | 0.756 | 0.719 | 1.754 | | | | |
| 360 | 0.731 | 0.700 | 1.735 | | | | |

extremes from eq. (2). The values of $m$ could not be determined with certainty using eq. (2). A few sets of values were tried, and $d_2$ was calculated. The set of values of $m$ that gave the smallest dispersion in the average value of $d_2$ is shown in Table V. The average value of $d_2$ in Table V is 2504 ± 44 nm. Using the accurate values of $m$ and an average $d_2$ value, $n$ can again be calculated for each λ using eq. (2). These values are shown as $n_2$ in Table V.

Now $n_2$ can be fitted to a function for extrapolation to shorter wavelengths. Using a function of the form

$$n = \frac{a}{\lambda^2} + c, \tag{7}$$

we obtained

$$n = \frac{2.101 \times 10^4}{\lambda^2} + 1.654 \tag{8}$$

Because $n(\lambda)$ is known from eq. (8) (see Fig. 8), $X(\lambda)$ can be determined from eq. (9), and $\alpha(\lambda)$ can be calculated from $X(\lambda)$ and $d$ using eq. (11). Swanepoel[19] recommended that $T_M$ with eq. (9) be used to calculate $\alpha$ over the entire range of the spectrum:

$$X = \frac{E_M - [E_M^2 - (n^2 - 1)^3(n^2 - s^4)]^{1/2}}{(n - 1)^3(n - s^2)}, \tag{9}$$

where

$$E_M = \frac{8n^2 s}{T_M} + (n^2 - 1)(n^2 - s^2) \tag{10}$$

**Table VI Values of $\alpha$**

| $\lambda$ (nm) | $T_M$ | $n$ | $E_M$ | $x$ | $\alpha$ (nm$^{-1}$) | $\alpha$ (cm$^{-1}$) |
|---|---|---|---|---|---|---|
| 774 | 0.893 | 1.700 | 41.26 | 0.984 | 2.77E−06 | 27.658 |
| 736 | 0.896 | 1.690 | 40.61 | 0.987 | 2.34E−06 | 23.405 |
| 708 | 0.897 | 1.696 | 40.88 | 0.989 | 2.01E−06 | 20.052 |
| 684 | 0.899 | 1.707 | 41.40 | 0.990 | 1.67E−06 | 16.699 |
| 654 | 0.899 | 1.697 | 40.86 | 0.991 | 1.65E−06 | 16.461 |
| 634 | 0.899 | 1.709 | 41.49 | 0.991 | 1.62E−06 | 16.161 |
| 612 | 0.901 | 1.711 | 41.53 | 0.992 | 1.39E−06 | 13.905 |
| 594 | 0.902 | 1.720 | 41.98 | 0.993 | 1.16E−06 | 11.638 |
| 574 | 0.899 | 1.719 | 42.06 | 0.991 | 1.62E−06 | 16.242 |
| 556 | 0.897 | 1.721 | 42.26 | 0.988 | 2.09E−06 | 20.852 |
| 540 | 0.895 | 1.725 | 42.61 | 0.986 | 2.48E−06 | 24.757 |
| 526 | 0.893 | 1.733 | 43.15 | 0.984 | 2.86E−06 | 28.647 |
| 510 | 0.892 | 1.731 | 43.10 | 0.982 | 3.08E−06 | 30.779 |
| 498 | 0.891 | 1.740 | 43.67 | 0.981 | 3.28E−06 | 32.849 |
| 486 | 0.888 | 1.747 | 44.19 | 0.978 | 3.80E−06 | 38.035 |
| 472 | 0.885 | 1.743 | 44.14 | 0.975 | 4.33E−06 | 43.305 |
| 462 | 0.881 | 1.752 | 44.85 | 0.972 | 4.99E−06 | 49.859 |
| 452 | 0.878 | 1.760 | 45.45 | 0.968 | 5.64E−06 | 56.438 |
| 440 | 0.873 | 1.757 | 45.56 | 0.962 | 6.68E−06 | 66.804 |
| 432 | 0.867 | 1.768 | 46.51 | 0.957 | 7.70E−06 | 77.046 |
| 422 | 0.860 | 1.769 | 46.98 | 0.948 | 9.17E−06 | 91.742 |
| 414 | 0.852 | 1.777 | 47.87 | 0.940 | 1.06E−05 | 106.436 |
| 406 | 0.842 | 1.783 | 48.78 | 0.930 | 1.25E−05 | 124.969 |
| 398 | 0.833 | 1.788 | 49.62 | 0.920 | 1.44E−05 | 143.724 |
| 390 | 0.820 | 1.791 | 50.58 | 0.906 | 1.70E−05 | 170.262 |
| 384 | 0.807 | 1.802 | 52.10 | 0.893 | 1.97E−05 | 196.936 |
| 376 | 0.793 | 1.802 | 52.93 | 0.879 | 2.24E−05 | 224.205 |
| 370 | 0.780 | 1.810 | 54.35 | 0.865 | 2.52E−05 | 251.566 |

and

$$\alpha = -\frac{\log X}{d} \tag{11}$$

The values of $\alpha$ at the extremes are shown in Table VI.

Once $\alpha(\lambda)$ is known, the extinction coefficient $k(\lambda)$ can be calculated from

$$k = \frac{\alpha\lambda}{4\pi}, \tag{12}$$

which completes the calculation of the optical constants.

To determine the influence of the dispersion relation $\tilde{\chi}^{(L)}(\lambda)$ of the (generally complex) linear susceptibility tensor on the dispersion $\tilde{\chi}^{(2)}(\lambda)$ of the (second-order) nonlinear susceptibility tensor, we refer[20] to the s.c. Miller's rule:

$$\frac{\chi^{(2)}_{ijk}\left(\frac{1}{\lambda_1}+\frac{1}{\lambda_2};\ \lambda_1,\ \lambda_2\right)}{\chi^{(L)}_{ii}\left(\frac{1}{\lambda_1}+\frac{1}{\lambda_2}\right)\chi^{(L)}_{jj}(\lambda_1)\chi^{(L)}_{kk}(\lambda_2)} = \delta \approx \text{const.} \tag{13}$$

The magnitude of the parameter $\delta$ can be estimated on the basis of the first-order perturbation theory of the Lorentz model. Practically, for a large class of optical materials, this parameter is found to vary no more than 100%.[21] In practice, instead of using the dispersion relation $\tilde{\chi}^{(L)}(\lambda)$, it is more convenient to use the dispersion of the refractive index $n(\lambda)$ and decay constant $k(\lambda)$, which are defined[19] by the s.c. complex refractive index $\mathbf{n}(\lambda) = n(\lambda) - ik(\lambda)$ as

$$\mathrm{Re}[\tilde{\chi}^{(L)}(\lambda)] = \mathrm{Re}[\mathbf{n}^2(\lambda) - 1] = n^2(\lambda) - \alpha^2(\lambda) - 1,$$

$$\mathrm{Im}[\tilde{\chi}^{(L)}(\lambda)] = -2n(\lambda)k(\lambda) \quad i = x, y, z. \tag{14}$$

As an example, we determine the dispersion relation $\tilde{\chi}^{(2)}(\lambda)$ of the nonlinear susceptibility tensor for the degenerated second-harmonic generation process ($o + o \rightarrow e$) in an uniaxial birefringent nonlinear crystal ($n_{xx} = n_{yy} = n_o$, $n_{zz} = n_e$, $k_{xx} = k_{yy} = k_o$, $k_{zz} = k_e$). According to Miller's rule in eq. (13), we obtain the dispersion relation for the real and imaginary parts of the nonlinear susceptibility tensor element $\chi^{(2)}_{xyy}$ as follows:

$$\begin{aligned}\mathrm{Re}[\chi^{(2)}_{xyy}(\lambda)] = \mathrm{Re}[&\delta(n_e^2(\lambda) - k_e^2(\lambda) - 1 - i2n_e(\lambda)k_e \\ &\times (\lambda))(n_o^2(2\lambda) - k_o^2(2\lambda) - 1 - i2n_o(2\lambda)k_o(2\lambda))^2]\end{aligned}$$

and

$$\begin{aligned}\mathrm{Im}[\chi^{(2)}_{xyy}(\lambda)] = \mathrm{Im}[&\delta(n_e^2(\lambda) - k_e^2(\lambda) \\ &- 1 - i2n_e(\lambda)k_e(\lambda))(n_o^2(2\lambda) \\ &- k_o^2(2\lambda) - 1 - i2n_o(2\lambda)k_o(2\lambda))^2] \quad (15)\end{aligned}$$

## CONCLUSIONS

This article explored the synthesis of polyarylates with side-chain groups based on new compounds 2,4-dihydroxybenzaldehyde and formyl bisphenol A derivatives as a special monomers and bisphenol A. Formyl bisphenol A was synthesized using the Reimer–Tiemann method. Six new special monomers containing thiazol heterocyclic rings and azometine groups were synthesized. The conditions of the synthesis of monomers and polymers were optimized. Structures of products were confirmed by $^1$H-NMR, IR, and MS.

Fourteen polyarylates were synthesised by interfacial polycondensation reaction using TEBA-Cl as a catalyst. Special monomers were used in 1–10 mol % in mixture with bisphenol A. Two monomers (1c and 2d, see Fig. 1) were hydrolyzed during the polycondensation reaction in basic conditions of reacting mixture, and most probably polymers with formyl side-chain groups were obtained.

The values of intrinsic viscosity of obtained polymers were found to be 0.74–1.98 (100 cm$^3$/g). This means that polymers had high molecular weights. Obtained polymer films had good mechanical properties, with tensile strength values of 20–60 MPa. All polymers showed high thermic resistance. Polymers with higher concentration of special monomer decomposed a little easier. However, polymers showed a high glass temperature typical for aromatic polyesters.

Several optical constants were calculated for polymer PAr **1a** 2% film. The thickness of polymer film was also calculated with good accuracy. The uniform films of these materials can be characterized and shown to be useful for applications in optical devices.

## REFERENCES

1. Prasad, N.; Ulrich, D. R. Non-Linear Optical and Electroactive Polymers; Plenum Press: New York, 1988.
2. Burland, D. M. Chem Rev 1994, 94, 31–75.
3. Nuken, O. Prog Polymer Sci 1997, 22, 93–183.
4. U.S. Pat. 4,978,479, 1990.
5. Brzozowski, Z. K.; Jóźwik, B. Photochem 1986, 35, 341–352.
6. Brzozowski, Z. K.; Zadrożna, I.; Lato, E. Polym Compos 1994, 2, 253A–258A.
7. Brzozowski, Z. K.; Kamiński, R. Makromol Reports A 1994, 31, 1, 217–223.
8. Brzozowski, Z. K.; Szymańska, E. Makromol Reports A 1994, 31, 643–650.
9. Brzozowski, Z. K. Polimery [English] 1984, 29, 10–12, 415–421.
10. Noniewicz, K.; Brzozowski, Z. K.; Zadrożna, I. J Appl Polym Sci 1996, 60, 1071–1082.
11. Brzozowski, Z. K.; Zadrożna, I.; Kowalczyk, T.; Syromyatnikov, V. S. Polym Polym Compos 1995, 3, 421.
12. Zadrożna, I.; Brzozowski, Z. K.; Noniewicz, K.; Dyrda, M. Polym Polym Compos 1997, 5, 57.
13. Brzozowski, Z. K.; Zadrożna, I. XIII European Experimental NMR Conference, Paris, May 1996.
14. Polish Standards PN-81/C-89092, PN-61/EO4403, PN-61/EO4405.
15. Vogel, A. I. Textbook of Practical Organic Chemistry Including Qualitative Organic Analysis, PWN; Warsaw, 1984.
16. Morgan, P. W. Condensation Polymers by Interfacial and Solution Methods; Interscience: New York, 1965.
17. Brzozowski, Z. K.; Zadrożna, I. International Symposium on Polymers at the Phase Boundary, Lviv (Ukraine), 1994.
18. Morison, R. T.; Boyd, R. N. Organic Chemistry; PWN: Warsaw, 1990.
19. Swanepoel, R. J Phys E: Sci Instrum 1983, 16, 1214–1222.
20. Boyd, R. Nonlinear Optics; Academic Press: New York, 1992.
21. Butcher, P.; Cotter, D. The Elements of Nonlinear Optics; Cambridge University Press: Cambridge, UK, 1990.